

Measurement Accuracy on Indoor Positioning System Using SS Ultrasonic Waves for Drone Applications

Tatsuki Okada

Graduate school of Software and
Information Science
Iwate Prefectural University
020-0693,Sugo Japan

Email: g231s004@s.iwate-pu.ac.jp

Akimasa Suzuki

Department of Information Science,
Iwate Prefectural University
020-0693,Sugo Japan

Email: suzuki_a@iwate-pu.ac.jp

Abstract—This study develops a drone positioning system for use in indoor environments, including in dark places, inaccessible areas, and ordinary living environments where it is difficult to realize by any conventional methods. Various indoor applications using drones have been developed for applications such as drone communication systems and wall surface inspection, which require remote estimation of their position. For outdoor applications, a Global Navigation Satellite System (GNSS) is generally used to obtain the drone position. However, as the radiowaves of the GNSS cannot reach indoors or between buildings, camera-based methods, such as Simultaneous Localization And Mapping (SLAM), are applied to estimate the drone's position. The system uses a noise-resistant, code-division-multiplexed Spread Spectrum (SS) ultrasonic waves for three-dimensional positioning. We develop transmitter and receiver hardware using SS ultrasonic waves and evaluate the effect of wind and sound of the positioning system during drone operations on the SS ultrasonic positioning. The accuracy of the positioning system was verified through experiments, and the results showed that a positioning accuracy within 15 cm was possible despite the effects of downwash generated by the drone's wings.

Keywords—Drone; Indoor Positioning System; SS Ultrasonic Waves; Downwash

I. INTRODUCTION

As Unmanned Aerial Vehicles (UAV), drones can be flown autonomously or operated by remote control. Because they can take off and land vertically in small spaces, they can be used to perform a variety of activities in unstable places where people and vehicles cannot enter. Previous studies have investigated the use of drones for autonomous search and rescue operations for victims following a disaster [1], meteorological observations [2], and logistics such as home delivery [3].

When used indoors, drones act as communication robots [4]. However, an appropriate distance is required to allow natural and smooth communication between a human and an autonomous mobile robot. To ensure the appropriate positioning in indoor spaces, the drone's coordinates can be used to develop real-time centimeter-order positioning. On the other hand, a relevant study investigated the use of drones for periodic inspections to detect aging degradation of locations where staff is unable to work, such as high walls of tanks and industrial chimneys [5]. Using drones to conduct periodic inspections is expected to reduce the high cost of these inspections.

It is more dangerous to use drones indoors than outdoors because it is easier to crash the drone into obstacles, such as humans and walls. Thus, it is essential to determine the position of the drone in relation to other objects. As horizontal and vertical relationships are important in these applications, it is essential to obtain absolute coordinates in space. While a Global Navigation Satellite System (GNSS) is generally used to obtain the absolute coordinates of a drone, the GNSS signal is difficult to detect indoors. Simultaneous Localization and Mapping (SLAM) is often used in non-GNSS environments. However, the flight path of a routine inspection is often in a dark place and the walls do not always follow a uniform pattern, causing large errors in SLAM's self-position estimation.

We therefore propose an indoor positioning system for drones using spread spectrum (SS) ultrasonic waves [6]. This system is expected to obtain 3D coordinates with an accuracy of 10cm. However, noise from the propellers or downwash of a drone may lower this accuracy. Downwash is the wind created by the drone's propellers. Therefore, this study conducts an experiment to evaluate the positioning accuracy of drone flights during a periodic inspection. Section II presents related research. Section III presents an overview of indoor positioning systems using SS ultrasound. Section IV presents the experiments and their results.

II. RELEVANT STUDIES AND PREVIOUS WORKS

There is no positioning method with drones for indoor multi environments, including dark environments with accuracy under 10 cm. Various sensor systems have been investigated for indoor positioning purposes, including pseudolites [7] and beacons [8]. Of these, ultrasonic-wave-based systems have lower cost and greater accuracy. However, because these systems use the time-division multiplexing method with on-off keying, which grows increasingly cumbersome as the number of objects to be measured grows, they generally have weak noise resistance and are slow to acquire data. Systems using SS ultrasonic signals have therefore been investigated to overcome these drawbacks [9] [10].

Analogous to SS radiowave systems (e.g., GPS), we have proposed a real-time 3D positioning system using SS ultrasonic signals with a band-limited transducer, A Low-Power Field Programmable Gate Array (FPGA), and a small microprocessor [11] [12]. In previous studies, we discussed factors such as positioning errors in indoor environments [6] and signal

degradation with band-limited transducers [13] and showed the measurement accuracy of the positioning system using SS ultrasonic signals. We also proposed a calculation algorithm based on the Newton–Raphson method for continuous signals, rather than conventional pulse signals. As a result, 3D coordinates can be obtained every 80ms using Code Division Multiple Access (CDMA) with continuous signals [14].

We evaluated the positioning accuracy of SS ultrasonic waves using a ground-based mobile robot [15]. Other studies have proposed using not only SS ultrasonic waves but also image sensors for drone positioning [16] and applying drones to limited situations such as a greenhouse [17]. Indoor positioning accuracy has been discussed using the Kinect camera, the average positioning error was 48mm [18]. However, it is difficult to use in the dark. This study develops an indoor positioning system using only SS ultrasonic waves that can be used in dark places where image sensors are ineffective.

III. INDOOR DRONE POSITIONING SYSTEM USING SS ULTRASONIC SIGNALS

This section describes the indoor positioning method using SS ultrasonic waves and our proposed system.

A. A method for positional calculation

Figure 1 presents the positioning calculations for the indoor positioning system using SS ultrasonic waves. Spheres are drawn to determine the center point on the radius between a receiver R_c and each transmitter, and two pairs of spheres are selected centering on Tr_1 and Tr_3 , and Tr_2 and Tr_3 , respectively. From these pairs of spheres, $Plane_{13}$ and $Plane_{23}$ are solved as a simultaneous equation and a line of intersection is obtained from the two planes. Last, the points at the intersection of the line with an equation of an arbitrary sphere are solved. Figure 2 also shows a flowchart of the algorithm for the positioning calculation in Figure 1. Two intersection points are obtained transmitters are installed along the wall; therefore, one solution becomes outside of the room. Thus, the other solution becomes the position of the receiver R_c . When using four transmitters, four position results are obtained. Thus, the measurement position is defined as an average of these results.

B. Hardware structure of a positioning system using SS ultrasonic waves

A 3D position can be calculated on the basis of three or more Times Of Flight (TOF) between the transmitters and the receiver. Figure 3 shows the system architecture of the TOF measurement for the positioning system. The transmission unit contains a D/A converter and an FPGA to generate carrier waves and M-sequences. The reception unit includes an A/D converter and an FPGA for correlation calculation, peak detection, and time measurement.

An SS signal is generated by the transmission unit to multiple carrier waves by M-sequences and is outputted from a transducer after D/A conversions. At the start of the transmission, a time counter is started to measure the TOF, and correlation values are calculated from the sound data via the A/D converter as online and real-time hardware processing. The time counter measures the TOF by counting the sampling times until arriving at peak correlation values, obtained by the peak detector. Then, the 3D position of the receiver can be calculated based on three or more TOFs between the

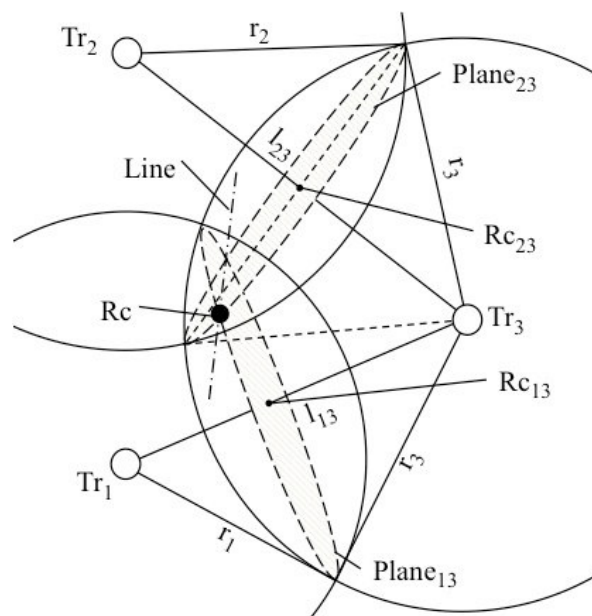


Figure 1. Positioning calculations for the indoor positioning system.

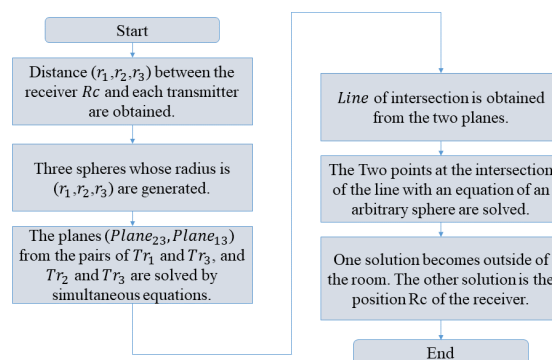


Figure 2. Flowchart on our position calculation

transmitters and receiver. The correlation calculator part is installed in the hardware as shown in Figure 3. Distance is obtained from the TOF obtained from the hardware and dimensional position is measured. Real-time positioning is enough available because this processing can be calculated lightly in software using optimized expressions.

C. SS signal

In our indoor positioning system, SS signals are modulated by binary phase shift keying using M-sequence, a pseudo-random code sequence, with a direct sequence method. Although the M-sequence of ‘0’ or ‘1’ is generated by a shift register, we replace a value of ‘-1’ with ‘0’ for easy signal processing. Figure 4 shows a received SS signal, where the signals corresponding to ‘1’ and ‘-1’ are plotted in solid and dashed lines, respectively. Each dot of Figure 4 is described as a sample convert to digital signal; the amount of sample including one period of carrier waves is decided on four samples. Here, chip length t_c is defined as the time required to describe 1-chip of the M-sequence; the chip length can also be described as $t_c = 4/f$ using carrier frequency f . The length of

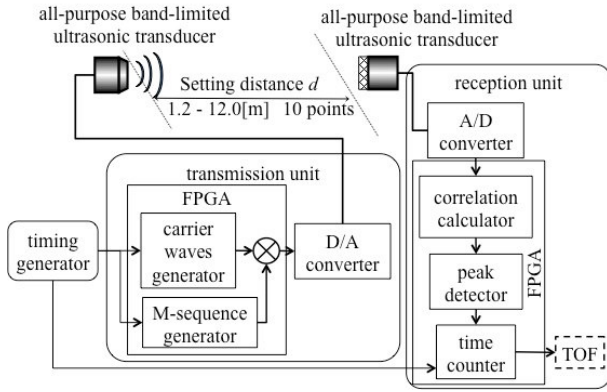


Figure 3. System architecture of the TOF measurement.

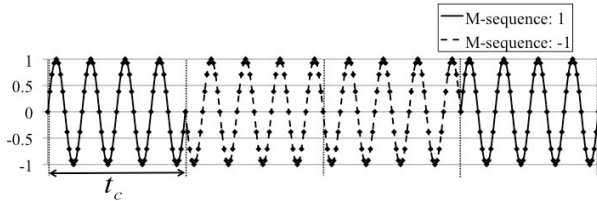


Figure 4. Spread spectrum ultrasonic signal.

SS ultrasonic signals becomes $2^9 - 1 = 511$ [chip] due to a 9-bit shift register for the M-sequence in our system. These four channels of the transmitters are generated by the following tap positions: $\{4,9\}$, $\{3,4,6,9\}$, $\{4,5,8,9\}$, and $\{1,4,8,9\}$. In this system, the frequency of the carrier waves is 40.2kHz.

D. Our proposed indoor positioning system using SS ultrasonic for drones

In this system, we use a transmitter with a closed-type aperture (PC40-18S, Nippon Ceramic Co., Ltd.) and a “Mini” SiSonic™ ultrasonic receiver (SPM0404UD5, Knowles) as general-purpose ultrasonic transducers.

Figure 5 shows the layout of the transmitters and receiver for our proposed system. We use two example situations, a dark plant and a room, as shown in Figures 5(a) and 5(b), respectively. Figure 5(a) represents a periodical inspection at a plant, where it is difficult to install infrastructure, such as transmitters, in the building. Transmitters are therefore set on a cross-shaped mount, as shown in Figure 5(a), for convenient mounting. Considering the Dilution Of Precision (DOP), the larger the mount size, the more accurate the expected positioning accuracy, although a larger size limits the installation position options and is inconvenient to carry. Figure 5(b) represents a communication drone. Transmitters are mounted in four corners of a room. In this situation, the transmitters are more difficult to install, but the DOP is better than the situation in Figure 5(a). In this paper, we conduct experiments using the layout shown in Figure 5(a).

The drone is fitted with a microphone and small receiving hardware, which processes the ultrasonic waves. Figure 6 illustrates the hardware schematic mounted on the drone. The hardware consists of an Evaluation Board (ACM204-1158C) installed in the FPGA (Intel Cyclone IV); a transceiver for timing the synchronization of the ultrasonic transmitter unit; a receiver unit; a USB interface for output coordinates; an input part to receive the ultrasonic waves, including an A/D converter

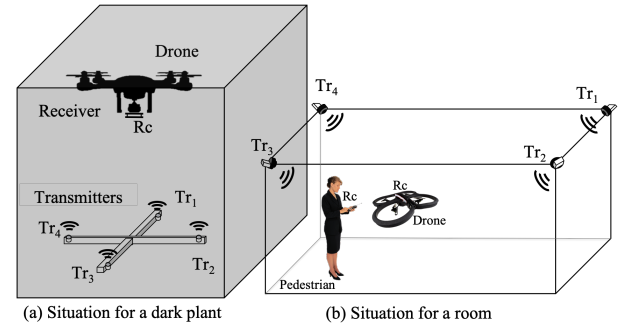


Figure 5. Measurement layout for the proposed system for (a) a dark plant and (b) a room.

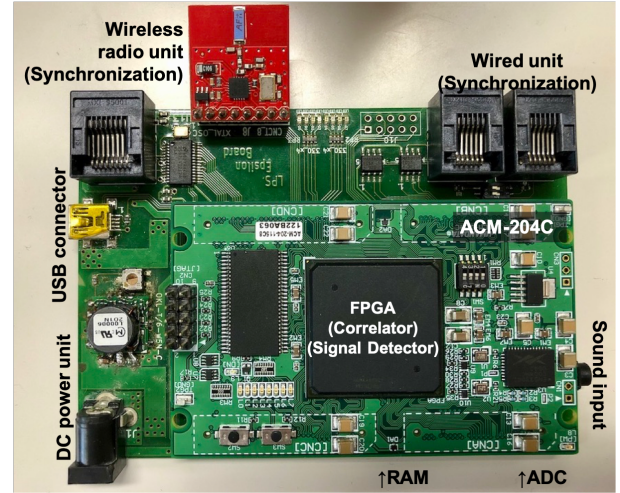


Figure 6. Receiving hardware for the drone measurements.

and amplifier; and SD-RAM for the real-time correlation calculations.

The USB interface and input part are connected to a computer and a microphone, respectively. Ultrasonic waves received by the microphone are converted to A/D and input into the FPGA, where the correlation calculations, peak detection, and TOF calculations are performed. The SD-RAM processes the real-time correlation calculations, and the transceiver measures the TOF based on the transmission timing received from the ultrasonic transmitter. Finally, the drone obtains the TOF by USB UART/FIFO IC (FTDI FT232H).

IV. POSITIONING ERROR BY DRONE NOISE AND DOWNWASH

We conducted experiments to evaluate the effect of motor noise, wind noise, and downwash generated by the propellers during flight on the SS ultrasonic positioning. Figure 7 shows the environment used for this experiment, which was a room 2000mm long and 4000mm wide. We used a Mavic 2 zoom by DJI™ drone for this experiment. Four transmitters Tr_1 – Tr_4 were placed near the center of the room. As shown in Figure 7, the drone’s starting point was the floor at the left front edge of the room. The coordinates of the transmitters were Tr_1 [mm] = (500, 2000, 1500), Tr_2 [mm] = (1000, 1500, 1500), Tr_3 [mm] = (1500, 2000, 1500), and Tr_4 [mm] = (1000, 2500, 1500). The transmitting SS signal was amplified to $50V_{p-p}$.

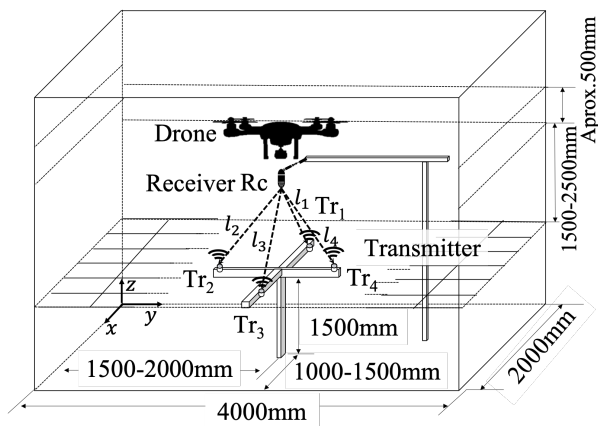


Figure 7. Layout for the positioning experiment.

Figure 8 shows the experimental environment. SS Ultrasonic waves are transmitted upward from Tr_1 – Tr_4 mounted on a tripod, and received by Rc , mounted on a bridge of wood.

Figure 9 shows the measurement point. The white and black circles in Figure 9 denote the transmit and receive points, respectively. $Rc_{(1000,2000,3000)}$ [mm], $Rc_{(1000,2000,3500)}$ [mm], and $Rc_{(1000,2000,4000)}$ [mm] are the receiving points at the center of the x – y plane of the four transmitters, located 1500mm, 2000mm, and 2500mm above the transmitters, respectively. Of the other receiving points, $Rc_{(1000,1500,3000)}$ [mm] and $Rc_{(1000,1500,4000)}$ [mm] are above transmitter Tr_2 and $Rc_{(500,2000,4000)}$ [mm] is above transmitter Tr_1 .

l_1 , l_2 , l_3 , and l_4 , which are the distances between the transmitters and a receiver (Figure 7), are measured for each receiving point. The drone is made to hover at a position approximately 500mm above the receiver. We examine the accuracy when the drone is in flight and when the drone is not in flight in the environment. Five trials were conducted for each receiving point.

A. Measurement error in distance

Figure 10 shows the average differences in the distances from the hovering drone for five trials. The vertical and horizontal axes on each graph denote the difference in distance from the drone compared to the measured distance from l_1 to l_4 to Tr_1 to Tr_4 , respectively. The differences in distances are shown as absolute values, and the average difference in the distance is shown as a black line.

The results of the experiment show that all measured distances are obtained when the drone is flying, but the measurement distance is affected by the drone's flight. Figure 10(a) shows the drone's distance for the four transmitters, where the receiving point is on the center of the x – y plane. A greater distance between the transmitter and receiver indicates larger measurement distance. Figure 10(b) compares the accuracy of the distance measurement at the center position (1000, 2000) with that when the drone is above Tr_2 at heights of 3000mm and 4000mm. The difference in distance measurement above Tr_2 is the same as that shown in Figure 10(a). Especially the difference in the distance between Tr_2 and $Rc_{(1000,1500,4000)}$, where above Tr_2 , is increased by the drone hovering. Figure 10(c) shows the measurement distance at the height of 4000mm, which shows that the difference in the distance

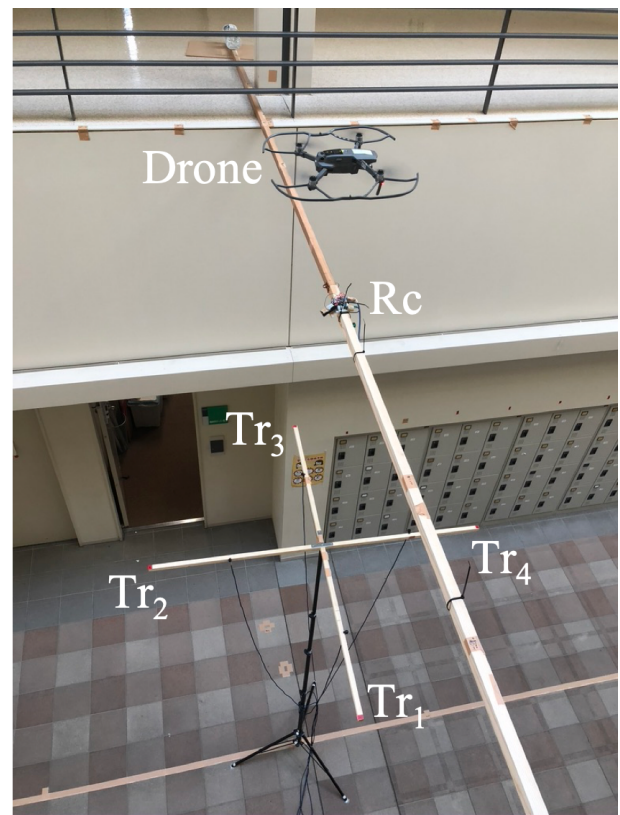


Figure 8. A view of the experiment from above.

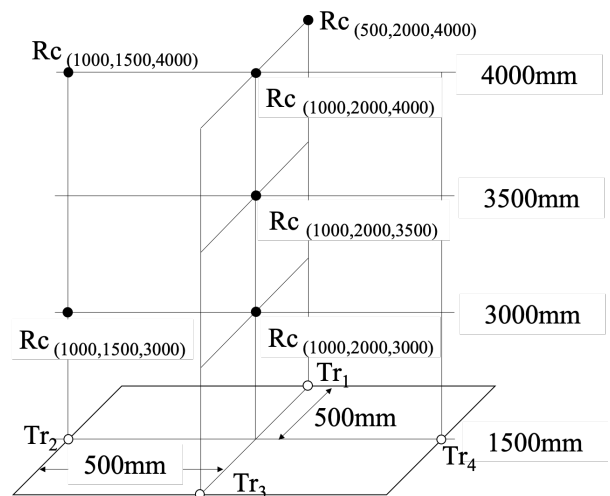


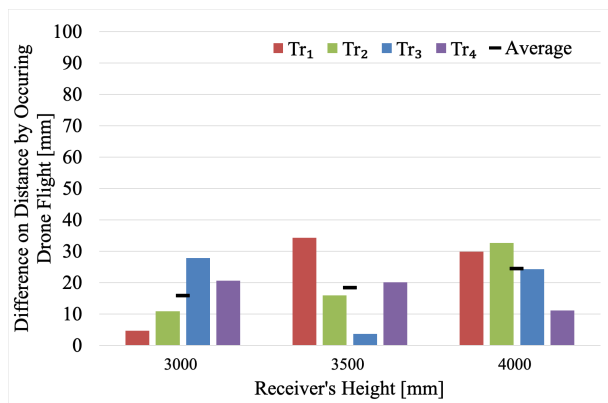
Figure 9. Measurement points of the receivers.

between Tr_1 and $Rc_{(500,2000,4000)}$ increases. Compared to $Rc_{(1000,2000,4000)}$, however, the average difference decreases.

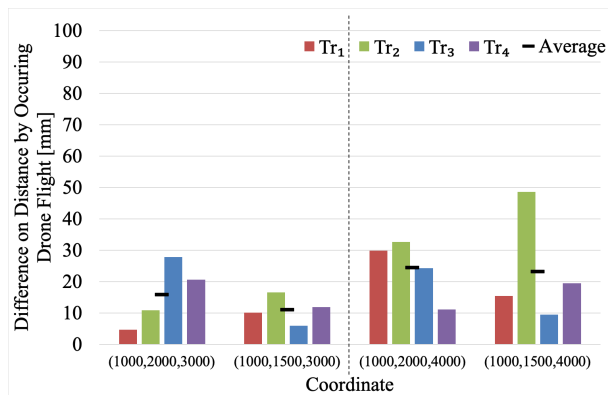
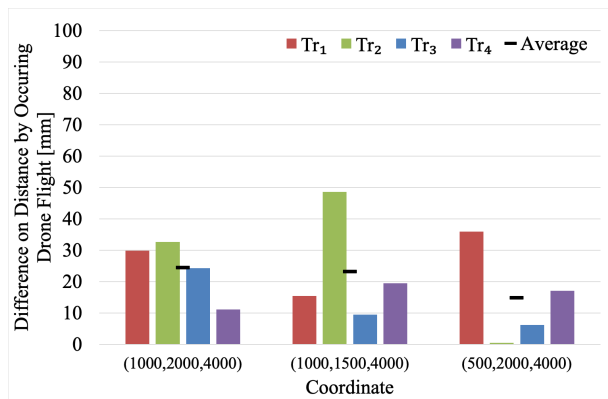
These graphs indicate that a drone's downwash and noise have a significant effect on the measurement distance when the transmitter and receiver are facing each other. The difference in the measured distance with and without drones is within 5cm.

B. Positioning Error

The experimental results were evaluated using the Root Mean Square (RMS) of the difference between the results and



(a) at each receiver's height on the center position


 (b) center position vs. above Tr₂


(c) at height of 4000mm

Figure 10. Difference in the measured distance occurred by drone flight.

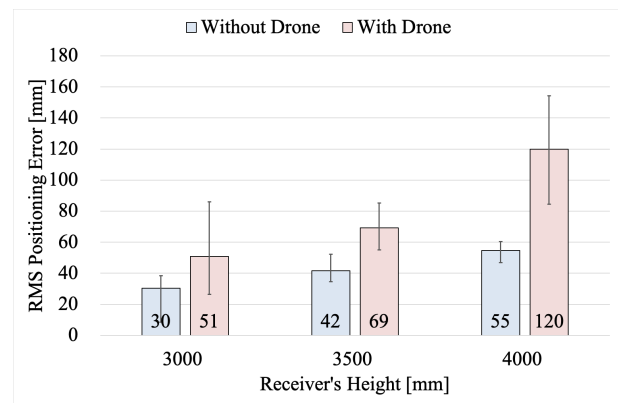
the installed distances. em_{rms} is defined as

$$em_{rms} = \sqrt{(dm_i - d_i)^2} \quad (1)$$

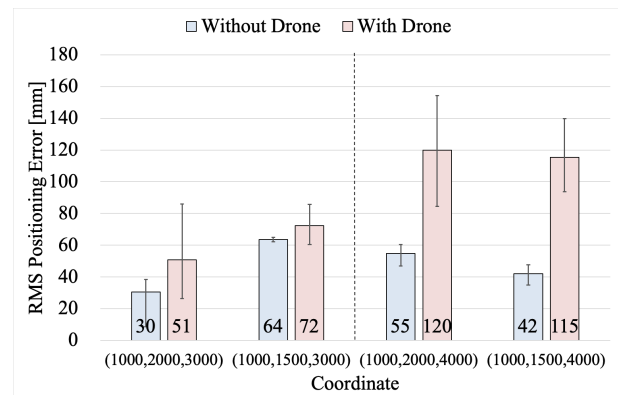
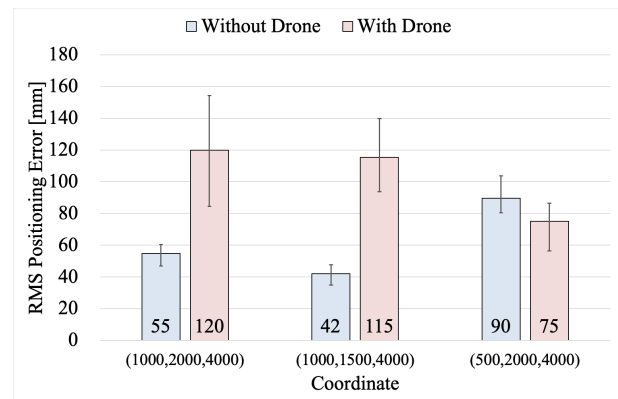
where d_i and dm_i are the measured distance and the true distance between a receiver and i -th transmitter, respectively.

Figure 11 shows RMS positioning errors at the same receivers shown in Figure 10 and the maximum and minimum positioning errors as "an expression" of variance. The vertical and horizontal axes of Figure 11 denote the RMS positioning error and the receiver coordinates, respectively. The positioning errors are an average of five trials.

These results indicate that the positioning error increased when the drone is flying because of downwash and flight noise;



(a) at the center position


 (b) on center position vs. above Tr₂


(c) at a height of 4000mm

Figure 11. RMS positioning error.

however, the average errors are less than 15cm. The results of Figures 11(a) and 11(b) confirm that the greater the distance between the transmitter and receiver, the larger the average RMS positioning error and variance when the drone was being flown. Figure 11(c) shows that the most variance is observed at the center of (1000, 2000, 4000).

The results of the experiment indicate that the transmission is accurate enough to measure a drone for a periodic inner wall inspection. We can expect more accurate positioning by compensating for errors caused by the angle of the transmitter and receiver and by the measurement distance [19].

V. CONCLUSIONS

This study proposed a positioning system using SS ultrasonic waves for indoor applications, such as drone communication and wall surface inspection, and evaluated the effects of the system against drone downwash and noise. The proposed SS ultrasonic positioning system transmits and receives SS signals using M-sequence, and the distance is measured using the TOF method. This study mounted small hardware and wideband microphones on the drone. The experimental results for assuming an inner wall inspection by the drone shows that downwash increases the positioning errors, but the errors are less than 15cm. We can expect greater accuracy in the layout of a communication robot because of low DOPs. Therefore, our positioning system using SS ultrasonic waves can be applied for drone application. We will examine the errors in positioning with multiple drones and discuss their errors occurred by flight noise and downwash.

ACKNOWLEDGEMENTS

This work was supported by MEXT KAKENHI Grant Number JP 10609423 and Foster Electric Company, Limited. We would like to thank Uni-edit (<https://uni-edit.net/>) for editing and proofreading this manuscript.

REFERENCES

- [1] L. Aprville, T. Tanzi, and J.-L. Dugelay, "Autonomous drones for assisting rescue services within the context of natural disasters," in 31st URSI General Assembly and Scientific Symposium, Beijing, China, Aug 2014, pp. 1–4.
- [2] A. E. MacDonald, "A global profiling system for improved weather and climate prediction," *Bulletin of the American Meteorological Society*, vol. 86, no. 12, Dec. 2005, pp. 1747–1764. [Online]. Available: <https://doi.org/10.1175/bams-86-12-1747>
- [3] W. Yoo, E. Yu, and J. Jung, "Drone delivery: Factors affecting the public's attitude and intention to adopt," *Telematics and Informatics*, vol. 35, no. 6, 2018, pp. 1687 – 1700. [Online]. Available: <http://www.sciencedirect.com/science/article/pii/S0736585318300388>
- [4] U. Nagarajan, G. Kantor, and R. L. Hollis, "Human-robot physical interaction with dynamically stable mobile robots," *Proceedings of the 4th ACM/IEEE international conference on Human robot interaction - HRI '09*, Mar 2009, p. 281–282. [Online]. Available: <http://dx.doi.org/10.1145/1514095.1514176>
- [5] F. Cunha and K. Youcef-Toumi, "Ultra-wideband radar for robust inspection drone in underground coal mines," in 2018 IEEE International Conference on Robotics and Automation (ICRA), Brisbane, Australia, Mar 2018, pp. 86–92.
- [6] A. Suzuki, T. Iyota, Y. Choi, Y. Kubota, K. Watanabe, and A. Yamane, "Measurement accuracy on indoor positioning system using spread spectrum ultrasonic waves," 4th International Conference on Autonomous Robots and Agents, Feb 2009, pp. 294–297.
- [7] X. G. et al., "Doppler differential positioning technology using the bds/gps indoor array pseudolite system," *Sensors*, vol. 19, no. 20, Oct 2019, p. 4580. [Online]. Available: <http://dx.doi.org/10.3390/s19204580>
- [8] D. Kudou, M. Horikawa, T. Furudate, and A. Okamoto, "Indoor positioning method using proximity bluetooth low-energy beacon," in *Proceedings of the 17th Asia Pacific Industrial Engineering and Management Systems Conference (APIEMS2016)*, Taiwan Taipei, Dec 2016.
- [9] M. Hazas and A. Hopper, "Broadband ultrasonic location systems for improved indoor positioning," *IEEE Transactions on Mobile Computing*, vol. 5, no. 5, 2006, pp. 536–547.
- [10] L. Segers, A. Braeken, and A. Touhafi, "Optimizations for FPGA-based ultrasound multiple-access spread spectrum ranging," *Journal of Sensors*, vol. 2020, Jun. 2020, pp. 1–26. [Online]. Available: <https://doi.org/10.1155/2020/4697345>
- [11] A. Suzuki, T. Iyota, and K. Watanabe, "A performance comparison of measurement distance between ook and ss modulation for indoor positioning using ultrasonic transducers," *IEEE Sensors*, Oct 2011.
- [12] —, "Real-time distance measurement for indoor positioning system using spread spectrum ultrasonic waves," in *Ultrasonic Waves*. InTech, Mar 2012. [Online]. Available: <https://doi.org/10.5772/30215>
- [13] A. Yamane, I. Taketoshi, C. YoungWoon, K. Yuzuru, and W. Kazuhiro, "A study on propagation characteristics of spread spectrum sound waves using a band-limited ultrasonic transducer," *Journal of Robotics and Mechatronics*, vol. 16, no. 3, 2004, pp. 333–341.
- [14] K. Kumakura, A. Suzuki, , and T. Iyota, "Indoor positioning for moving objects using a hardware device with spread spectrum ultrasonic waves," *International Conference on Indoor Positioning and Indoor Navigation (IPIN 2012)*, Nov 2012, pp. 1–6.
- [15] A. Suzuki, K. Kumakura, D. Tomizuka, Y. Hagiwara, Y. Kim, and Y. Choi, "Positioning accuracy on robot self-localization by real-time indoor positioning system with SS ultrasonic waves," *Journal of the Korea Society for Power System Engineering*, vol. 17, no. 5, Oct. 2013, pp. 100–111. [Online]. Available: <https://doi.org/10.9726/kspse.2013.17.5.100>
- [16] J. Paredes, F. Álvarez, T. Aguilera, and J. Villadangos, "3d indoor positioning of UAVs with spread spectrum ultrasound and time-of-flight cameras," *Sensors*, vol. 18, no. 2, Dec. 2017, p. 89. [Online]. Available: <https://doi.org/10.3390/s18010089>
- [17] Z. H. et al., "A noise tolerant spread spectrum sound-based local positioning system for operating a quadcopter in a greenhouse," *Sensors*, vol. 20, no. 7, Apr. 2020, p. 1981. [Online]. Available: <https://doi.org/10.3390/s20071981>
- [18] H. Zhang, G. Chen, Z. Wang, Z. Wang, and L. Sun, "Dense 3d mapping for indoor environment based on feature-point slam method," in *Proceedings of the 2020 the 4th International Conference on Innovation in Artificial Intelligence*, ser. ICI AI 2020. New York, NY, USA: Association for Computing Machinery, 2020, p. 42–46. [Online]. Available: <https://doi.org/10.1145/3390557.3394301>
- [19] A. Suzuki and T. Iyota, "Angular dependence of transducers for indoor positioning system using ss ultrasonic waves," 2012 International Conference on Indoor Positioning and Indoor Navigation, Nov 2012, pp. 1–6.